journal

J. Am. Ceram. Soc., 79 [10] 2601–608 (1996)

Freeform Fabrication of Ceramics via Stereolithography

Michelle L. Griffith*,† and John W. Halloran*

Department of Materials Science and Engineering, The University of Michigan, Ann Arbor, Michigan 48109-2136

Ceramic green bodies can be created using stereolithography methods where a ceramic suspension consisting of 0.40–0.55 volume fraction ceramic powder is dispersed within an ultraviolet-curable solution. Three ceramic materials were investigated: silica for investment casting purposes, and alumina and silicon nitride for structural parts. After mixing the powders in the curable solution, the ceramic suspension is photocured, layer by layer, fabricating a three-dimensional ceramic green body. Subsequent binder removal results in a sintered ceramic part. Three-dimensional objects have been fabricated from a 0.50 volume fraction silica suspension.

I. Introduction

FREEFORM fabrication involves shaping without the use of molds or tooling and has been accomplished with ceramics by selective laser sintering[1] and three-dimensional printing[2] techniques. Stereolithography (SL) is currently the most popular method for freeform fabrication,[3,4] but SL has not been used to produce ceramics. Stereolithography creates a solid body by scanning a laser beam on a liquid monomer, curing it in a line-by-line, layer-by-layer sequence.[5] Stereolithography machines or apparatuses (SLA), such as the SLA-250 and SLA-500 (3D Systems, Valencia, CA) are widely used with photopolymerizable polymers, including acrylates and epoxies. We have extended the stereolithography method so it can be used for freeform fabrication of ceramics, including structural ceramics such as alumina or silicon nitride and refractories such as silica-based shells and cores for investment casting. This is done via ultraviolet (UV) curing of a highly concentrated suspension of ceramic particles in a photopolymerizable liquid. The UV-curable liquid creates the polymer binder to form a net shape ceramic green part without the need of molds. The green part can be given a conventional binder burnout and sintering treatment.

"Stereolithography," invented by Chuck Hull,[6] was one of the first freeform fabrication technologies. This technique involves the polymerization of liquid monomers from exposure to ultraviolet radiation from a laser.[7] Figure 1 shows a schematic of the apparatus. With a stereolithography machine, a three-dimensional (3D) part is fabricated in a layer-by-layer process. First, a 3D computer image is sliced into many cross-sectional layers 150–200 μm thick. Using the information of each slice, laser radiation is scanned on the surface of the liquid monomer to draw the layer. As the laser scans the surface, the monomer is photocured to a polymer, where the polymerization depth is controlled by the radiation exposure (mJ/cm^2) and set to the layer thickness. When the layer is finished, the support platform and first layer move downward into the vat of liquid monomer resin. The liquid monomer flows across the first polymerized layer, and to ensure the second layer of monomer is of the desired thickness, a recoat blade moves across the surface. The laser scans this new surface, polymerizing the second layer. This process is repeated many times until the part is finished. When part building is done, the platform is raised and the solid polymer part emerges from the vat.

A candidate ceramic stereolithography suspension must satisfy several requirements. Since a high-quality ceramic is the goal, the freeform ceramic green body must have a high density, either for its refractory properties or so it can be readily sinterable to form a dense ceramic. The SLA suspension, at a 0.50–0.65 solids volume fraction, is a highly concentrated suspension, which must have a relatively low viscosity, preferably with no pronounced yield point. To operate in an SLA resin tank, the ceramic SLA suspension must be at least as fluid as conventional SLA resins (viscosity less than 3000 mPa·s) for proper flow during recoat of the new layer.[8] Obtaining effective dispersion for submicrometer powders requires careful design of the colloidal dispersant system. The viscosity of the pure monomer resin is extremely important. A lower starting viscosity usually results in a lower final viscosity for the suspension. Thus suspensions were prepared in low-viscosity UV-curable liquids, and dispersants were carefully selected to control the colloidal chemistry, and therefore the rheology.

The stereolithography apparatus builds parts from layers 150–200 μm thick. It is necessary that the cure depth of these highly loaded suspensions be equal to or greater than 150–200 μm after exposure to ultraviolet radiation in order to fabricate a ceramic green body in a sufficient amount of time. This concentrated ceramic suspension must be sufficiently transparent to ultraviolet radiation to permit an acceptable depth of cure. Powder suspensions can have a very high turbidity due to radiation scattering, even if the ceramic itself is transparent to UV. The scattering-induced turbidity limits the distance of penetration of the UV radiation into the suspension, and largely determines the depth of cure, C_d, for a ceramic suspension. The depth of cure can be modeled by assuming it to be the depth at which the UV beam is attenuated from the incident intensity (E_0) down to the minimum intensity required to achieve photocuring (E_c) for the particular photoinitiator/monomer system. This can be derived from the Beer–Lambert law:[9]

$$C_d \propto \frac{d}{\phi}\frac{1}{Q}\ln\left[\frac{E_0}{E_c}\right] \quad (1)$$

where the cure depth is proportional to the average particle

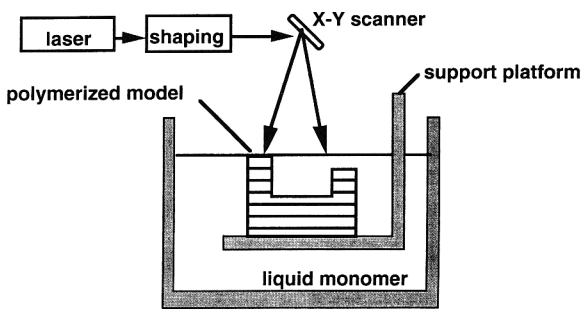

Fig. 1. Schematic of the 3D Systems' stereolithography apparatus (SLA) for fabrication of three-dimensional objects.

C. F. Zukoski—contributing editor

Manuscript No. 192329. Received September 11, 1995; approved March 28, 1996.
Supported by the Office of Naval Research under Grant No. N00014-913-1-0302.
*Member, American Ceramic Society.
†Now at Sandia National Laboratories, Albuquerque, New Mexico 87185.

Table I. Particle Size (d) and Refractive Index (n) for Ceramic Powders

Material	Density (g/mL)	d_{50} (μm)	d_{10} (μm)	d_{90} (μm)	Refractive index n at 366 nm
Silica†	2.65	2.29††	0.79	8.70	1.56
Silicon nitride‡	3.24	0.44‡‡	0.10	0.78	2.10
Alumina AKP-50§	3.96	0.46††	0.30	0.63	1.70
Alumina AKP-15§	3.96	0.61††	0.41	0.93	1.70
Alumina RC-HP¶	3.96	0.34‡‡	0.18	0.60	1.70

†α-quartz, Atlantic Equipment Engineering, Bergenfield, NJ. ‡UBE E10, UBE Industries, Tokyo, Japan. §AKP-15 and AKP-50 grades, Sumitomo Chemical, Tokyo, Japan. ¶RC-HP, Reynolds, from Malakoff Industries, Malakoff, TX. ††MICROTRAC particle size analyzer, Leeds & Northrop, North Wales, PA. ‡‡Particle size distribution analyzer, Model No. CAPA-700, Horiba, Irvine, CA.

size (d) and the logarithm of the exposure (E_0) and inversely proportional to the volume fraction ceramic (ϕ). The materials' scattering ability is described in the scattering efficiency term Q, where Q is a function of the refractive index difference between the ceramic and the UV-curable solution:

$$Q = \beta \Delta n^2 \tag{2}$$

Therefore, the cure depth is inversely proportional to $\Delta n^2 = (n_{ceramic} - n_{solution})^2$, where n is the refractive index. The term β is related to the particle size and the wavelength of the radiation, and this will be discussed later in the paper.

One important feature is the choice of the photoinitiator system. Photoinitiators react with the ultraviolet radiation and initiate polymerization. The absorptivity must be tuned to the particular UV wavelength and the concentration maximized for efficient photopolymerization through the depth of the suspension.[10]

The most important part of the SLA ceramic suspension is the ability to fabricate three-dimensional ceramic objects. Issues including shape integrity and adhesion between layers will be discussed.

II. Experimental Procedure

(1) Characteristics of the Ceramic Powders

Three ceramic materials were investigated in this research. Table I shows the particle size, density, and refractive index of the powders. Silica was chosen as a model material for investment casting applications. As is typical with investment casting refractory materials, the particle size was large and had a broad particle size distribution to improve the packing density. This silica powder was a milled quartz with a median particle size of 2.3 μm. The silicon nitride was a diimide-derived powder with a median particle size of 0.44 μm. Several alumina powders were used, including a high-purity ball-milled Bayer alumina (0.34 μm median, Reynolds' RC-HP) and two precipitated aluminas (0.46 and 0.61 μm, Sumitomo AKP-50 and AKP-15).

Table I also includes the refractive index information for silica,[11] silicon nitride,[11] and alumina.[12] The absorption edges are far below 313–370 nm UV wavelength range, so these three materials should be transparent to the UV radiation.

(2) Photopolymerizable Solutions

A photopolymerizable solution contains two or more materials. The minimum two materials are monomer(s) and photoinitiator(s). Nonreactive solvents may be added to reduce the viscosity, since most of the photomonomers have high viscosities, on the order of tens to thousands of mPa·s. Curing a monomer-solvent system creates a gel, which should have less polymerization shrinkage and easier binder removal upon firing.

The cured resin is the final product for conventional stereolithography, so cured resin properties are critical. For ceramic stereolithography, the photopolymer is only a binder for the ceramic particles in the green body, and the cured resin does not have to be very strong to impart adequate strength to the green ceramic. The polymer will later be removed, so its concentration should be minimized.

Two formulations of UV-curable solutions were examined: an aqueous acrylamide-based solution and a nonaqueous diacrylate. The aqueous acrylamide solution was a 9:1 mixture of acrylamide and methylenebisacrylamide in 0.50–0.70 volume fraction water, similar to a "gelcasting" formulation,[13,14] with the thermal initiators replaced with photoinitiators. This solution was further modified to vary the refractive index. Table II shows the refractive indices of the aqueous solutions, which were varied over the range 1.38–1.44 using mixtures of water (n = 1.33) and ethylene glycol (n = 1.43). The refractive index was measured by Abbey refractometry (Valentine Precision model, Industro Scientific, North Merrick, NY). The nonaqueous diacrylate is based upon the common monomer hexane diol diacrylate [HDDA], which is the 1–6 hexamethylene ester of acrylic acid (2-propenoic acid). The refractive index of the diacrylate is shown in Table II. This diacrylate is more viscous (6–12 mPa·s) than the aqueous media (1 mPa·s), but has a higher refractive index, and offers a good compromise between reactivity and low viscosity. It is similar to the usual acrylic ester-based monomers used in conventional stereolithography. Acrylate polymers are commonly used as ceramic binders.

(3) Preparing the Concentrated Ceramic Suspension

To prepare the suspensions, the UV-curable solution was prepared first, without the photoinitiators, and the ceramic powder (plus dispersants) was added incrementally. Up to about 0.30–0.35 solids loading, the suspension was mixed and homogenized in a high speed shear mixer. Above 0.35 volume fraction ceramic, more time was required for the dispersants to adsorb and colloidally stabilize the suspension, so ball milling was preferred for mixing and homogenization. When the maximum solids loading had been reached, the photoinitiators were added, and the suspension was ball-milled for 5 h to thoroughly mix the photoinitiators.

(4) Ultraviolet Curing of the Ceramic Suspensions

The curing behavior of the suspensions was first tested in a simple lamp apparatus (Hanovia UV Laboratory System, Hanovia, NJ). The ultraviolet curing apparatus consists of an ozone-free low-pressure mercury UV lamp enclosed in a housing with a conveyor belt to carry the samples under the lamp for exposure. The exposure dose of UV radiation was controlled with the conveyor speed and lamp setting, and measured with a radiometer (IL390B, International Light, Newburyport, NJ). The two main intensities of this UV lamp (313 and 366 nm) correspond to the laser intensities for the two SLA models

Table II. Refractive Index (n) and Viscosity for the Ultraviolet-Curable Solutions

Ultraviolet-curable solution	Refractive index (n)	Viscosity (mPa·s)†
Aqueous 1	1.382	~1
Aqueous 2	1.399	~1
Aqueous 3	1.415	~1
Aqueous 4	1.418	~1
Aqueous 5	1.441	~1
Diacrylate, HDDA	1.457	6

†Shear rate = 3 s^{-1}.

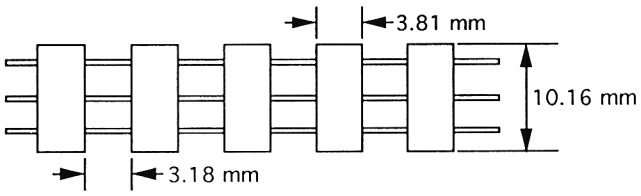

Fig. 2. Windowpane geometry showing five individual panes. Each pane receives a different exposure dose resulting in a different cure depth.

(313 nm for the He–Cd and 351 nm for the Ar ion). For the same exposure (mJ/cm^2), the lamp and laser produced similar cure depths.

A 2–3 mm thick layer of ceramic suspension in a petrie dish was passed through the apparatus and exposed to 100–5200 mJ/cm^2 ultraviolet radiation over a period of 2–10 s. After exposure, the polymerized layer was lifted off of the uncured suspension and rinsed. The cure depth was measured on the dried film by either optical or scanning electron microscopy.

Promising ceramic suspensions, with low viscosities and large cure depths, were tested in a stereolithography apparatus, Model SLA-250 with an Ar-ion laser (351 nm). For all ceramic suspensions, the first experiment was to fabricate "windowpanes" test parts,[15] illustrated in Fig. 2, to test for shape integrity. The laser scans the surface of the suspension to draw the three horizontal lines, followed by the outline of the "panes." Next the laser scans the interior of each pane at different scanning velocities so that each pane receives a different dose. After fabrication of the windowpanes, the cured part was removed from the rest of the uncured suspension and rinsed in either deionized water for the aqueous suspensions or ethanol for the acrylate suspension. Each windowpane thickness was measured with a micrometer to obtain the cure depth.

For three-dimensional parts, the stereolithography file 'Box' was used to fabricate a ceramic green body. Figure 3 shows the object, a hollow 2.54 cm (1 in.) cubed box with a 45° angle cut into one side. Before the box is fabricated, a support structure or scaffold is fabricated for easy removal of the 3D object from the support platform. The scaffold was designed by Bridgeworks (Solid Concepts, Valencia, CA) software.

III. Results and Discussion

(1) Viscosity of the Concentrated Ceramic Suspensions

All ceramic powders were easy to disperse in the aqueous UV-curable solutions. The colloidal chemistry is better understood for aqueous suspensions,[16–20] whether acidic (silica) or basic (alumina, silicon nitride) powders are chosen. Figure 4 shows the viscosity versus solids loading for silica dispersed in the lowest refractive index aqueous solution (aqueous 1).

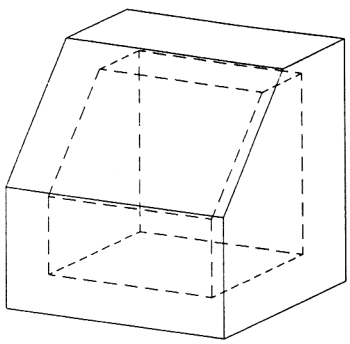

Fig. 3. Line drawing of the stereolithography file "box." The hollow box is 2.54 cm (1 in.) cube, with 3.2 mm (1/8 in.) wall thickness, and a 45° angle cut into one side.

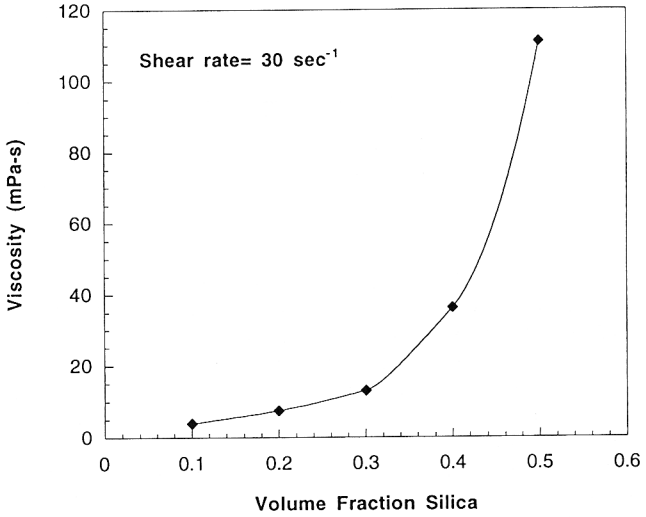

Fig. 4. Viscosity versus volume fraction silica added to aqueous solution 1 with $n = 1.382$.

As expected, the viscosity increases as the solids loading increases;[21] however, the suspension's viscosity at 0.50 solids loading is 120 mPa·s for a shear rate of 30 s^{-1}. This is well below the upper limit of 3000 mPa·s.

All suspensions are shear thinning, as shown in Fig. 5 for 50 vol% silica dispersed in two aqueous solutions (Nos. 1 and 4). The effective yield stresses for the aqueous suspensions are quite low, about 185 mPa, thereby promoting correct layer recoating. Table III shows the suspensions studied, the maximum solids loading, and the low shear rate viscosity of the ceramic suspensions.

The acrylate suspensions were exceedingly viscous, with viscosities greater than 3000 mPa·s for low shear rates at solids loadings less than 0.30. It is much more difficult to disperse ceramics in nonaqueous solutions,[22] but a 0.40 alumina solids loading in HDDA was achieved with a viscosity of 3000 mPa·s (shear rate = 6 s^{-1}).

(2) Ultraviolet Curing of Concentrated Ceramic Suspensions

For fabrication of ceramic green bodies via stereolithography to be feasible, the minimum cure depth per layer must be approximately 200 μm. Many users of the stereolithography apparatus cure polymer layers of 150 μm; this allows for smoother surfaces and finer features to be fabricated.

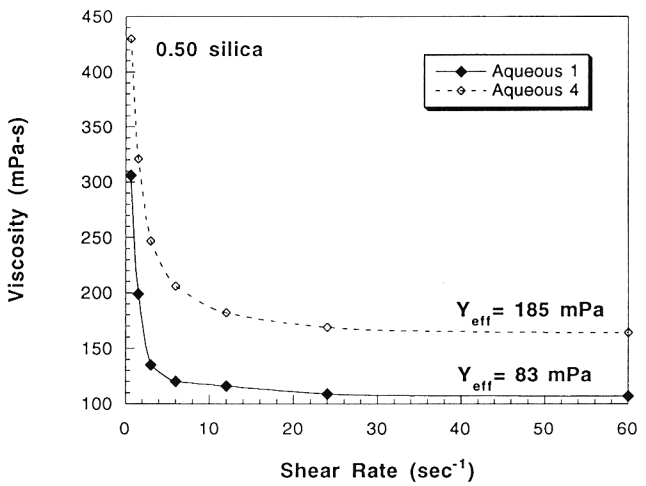

Fig. 5. Viscosity versus shear rate for 0.50 solids loading silica in two aqueous solutions, Aqueous 1 ($n = 1.382$) and Aqueous 4 ($n = 1.418$). Both suspensions have low yield point, Y_{eff}, values.

Table III. Maximum Solids Loading for Ceramic Suspensions and Corresponding Viscosities

Maximum solids ceramic	Ultraviolet-curable solution	Viscosity (mPa·s)†
0.50 silica (d = 2.29 μm)	All aqueous (n = 1.382–1.441)	200–500
0.50 alumina (d = 0.46 and 0.61 μm)	Aqueous 1 (n = 1.382)	500
0.40 alumina (d = 0.34 μm)	HDDA (n = 1.457)	3000

†Shear rate = 3 s^{-1}.

(A) Silica: Of the three materials, the cure depth of the silica suspensions should be the largest since silica has the smallest refractive index (n = 1.56). Figure 6 shows the cure depth versus inverse volume fraction silica added to the aqueous solution with a refractive index of 1.3824 (No. 1). As expected from the Beer–Lambert law and Eq. (1), the cure depth decreases as more silica is added to the suspension. At 0.50 solids loading of silica, the cure depth is greater than the minimum requirement, where C_d = 360 μm at an exposure dose of 1500 mJ/cm^2. Even at 0.55 volume fraction, the cure depth is above 200 μm, where C_d = 330 μm.

The cure depth is reasonable for 0.50 solids loading silica dispersed in the lowest refractive index solution, but a larger value would allow the SLA operator to choose the layer thickness. Figure 7 shows the cure depth versus dose for 0.50 solids loading of silica dispersed in a variety of aqueous UV-curable solutions. As the refractive index difference decreases from Δn^2 = 0.0317 to 0.0142, the cure depth increases from 250 to 700 μm for a dose of 1500 mJ/cm^2. A small change in refractive index for the UV-curable solution (4%) results in a 3-fold increase in the cure depth. Note, the cure depth versus the log of the exposure shows linear behavior as predicted from Eq. (1).

In stereolithography the dose is usually less than 500 mJ/cm^2. These low doses cannot be achieved with the lamp apparatus, and therefore it was necessary to study the cure depth behavior at low doses in an SLA. Figure 8 shows the cure behavior for two ceramic suspensions: 0.50 solids loading of silica added to an aqueous solution (n = 1.418) and 0.40 solids loading of alumina added to the diacrylate. At large doses, the cure depth is nearly the same as the lamp results for the silica suspension. Therefore, the lamp accurately models the cure behavior for these concentrated suspensions.

In Fig. 8, there are different regions of cure depth behavior. At doses above 300 mJ/cm^2, the cure behavior is linear and similar to the lamp results. For the silica suspension at doses lower than 300 mJ/cm^2, the cure depth has linear behavior, but with a different slope. For very low doses, less than 80 mJ/cm^2, the cure depth is most likely arrested by oxygen inhibition.[23] For the middle dose region, 80–300 mJ/cm^2, the cure behavior is more likely in an anaerobic condition,[24] where the polymerization rate strongly affects the cure depth as well as radiation scattering by the ceramic particles. At large doses, E_0 > 300 mJ/cm^2, the cure behavior is dominated by the scattering effects of the ceramic particles, whereas the photoinitiation rate saturates, producing enough free radicals for the polymerization

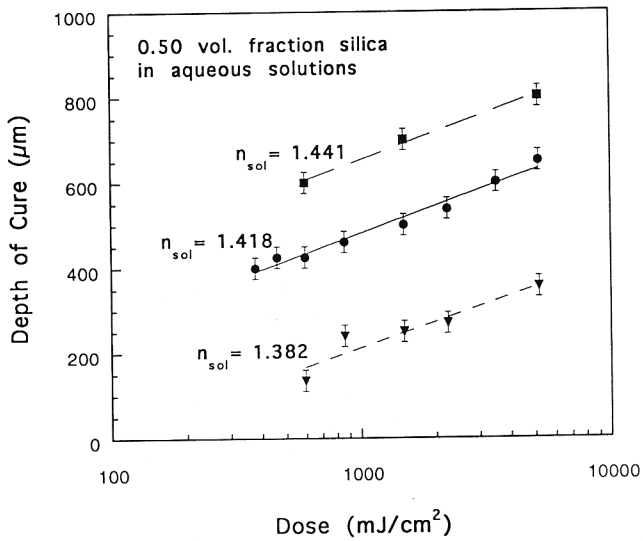

Fig. 7. Cure depth versus exposure dose for 0.50 volume fraction silica dispersed in three aqueous UV-curable solutions.

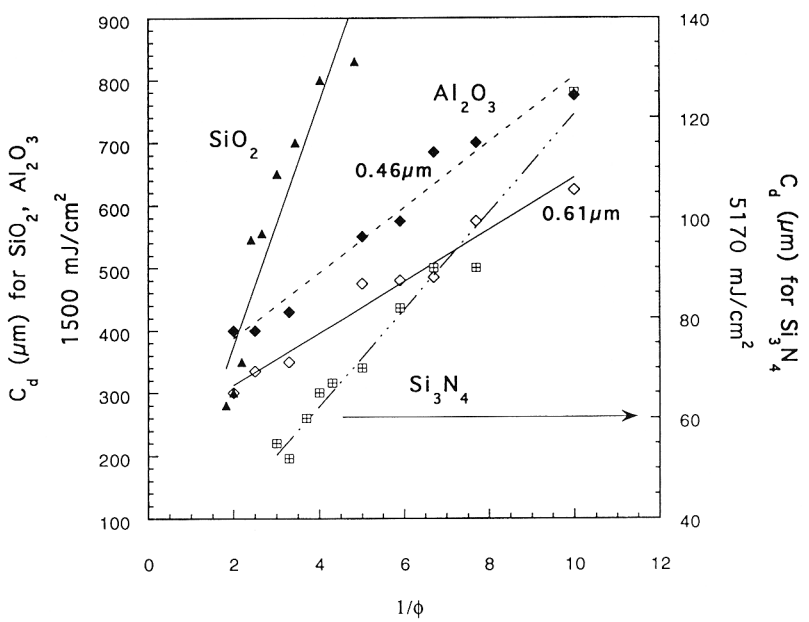

Fig. 6. Cure depth (C_d) versus volume fraction (1/1ϕ) for three ceramic suspensions, where all curves exhibit linear behavior. The silica and alumina powders are dispersed in the aqueous solution with a refractive index of 1.382 and the silicon nitride powder dispersed in the diacrylate.

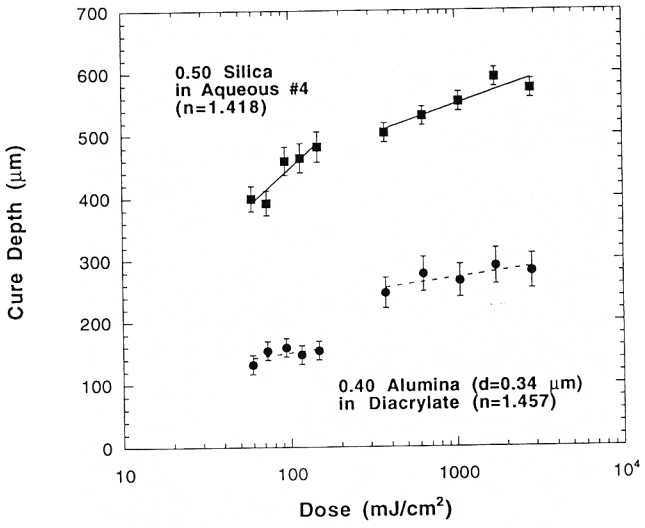

Fig. 8. Cure depth behavior over a wide exposure dose range for silica and alumina suspensions cured in stereolithography apparatus.

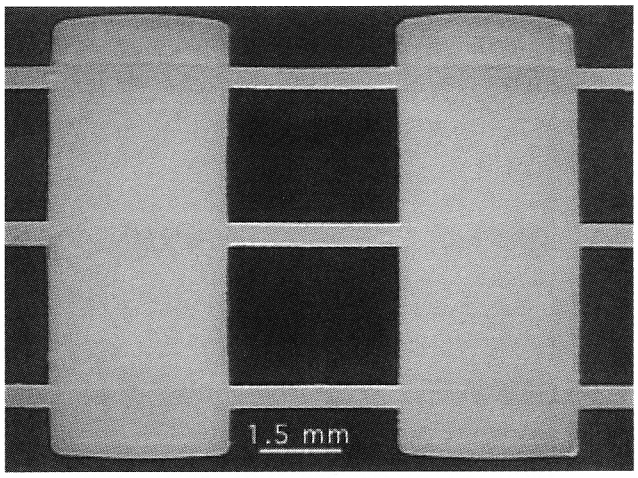

Fig. 9. Two representative panes built on SLA-250 with Ar-ion laser. Panes were fabricated from 0.40 volume fraction alumina (d = 0.34 μm) in the diacrylate.

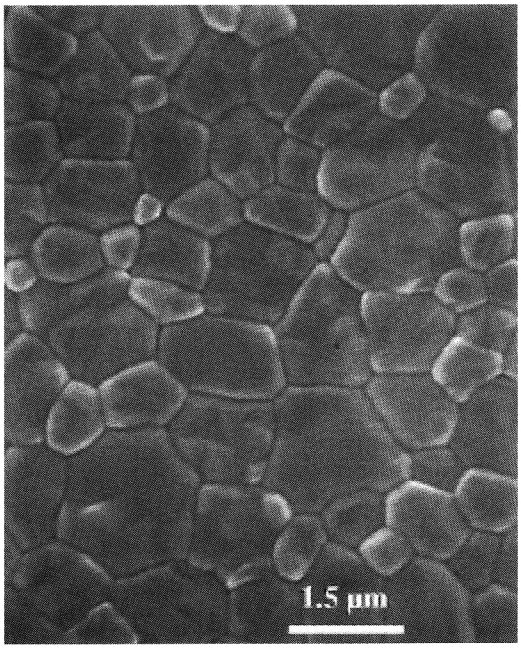

Fig. 10. Sintered alumina windowpane showing fully dense microstructure with grain sizes between 1 and 2 μm.

reaction, and is a secondary effect on the cure depth. The important point is the cure depth at doses as low as 50 mJ/cm^2 is still greater than 200 μm.

The alumina–diacrylate suspension shows a pronounced change in cure depth for doses less than 300 mJ/cm^2, similar to the silica–aqueous suspension. Oxygen inhibition most likely affects the low dose behavior for diacrylate solutions.[25,26]

(B) Alumina: Different grades of alumina were used in the UV-curable solutions to determine the effect of particle size on the cure depth. Figure 6 shows the cure depth versus inverse volume fraction alumina (two grades) added to the low refractive index aqueous solution (No. 1). At 0.50 solids loading and a dose of 1500 mJ/cm^2, both suspensions have cure depths greater than 200 μm. The smaller particle size alumina had a larger cure depth, 400 versus 300 μm. Table IV shows the results for different grades of alumina dispersed in a variety of aqueous UV-curable solutions, and particle size effects will be discussed later in this paper.

Windowpanes were fabricated from a 0.40 volume fraction alumina in the diacrylate solution. Figure 9 shows two representative panes from the windowpane. Note the spatial integrity with accurate laser lines and rectangular sections. The experimental panes are larger than the expected dimensions due to more side scattering in turbid suspensions. This error (5–15%) could be easily compensated for in the laser scanning pattern. Figure 8 shows the cure depth behavior for this suspension, where the necessary cure depth is achievable for doses larger than 300 mJ/cm^2. The green alumina windowpanes were slowly heated to 600°C to remove the polymers and then fired at 1550°C to sinter the alumina. Figure 10 shows the resulting microstructure of fully dense alumina.

Another requirement for stereolithography of ceramics is the layers must not be evident after firing of the green body. Figure 11(a) shows a sintered two-layer alumina part. The 0.40 volume fraction alumina in diacrylate suspension was tape cast with a thickness of 100 μm. The first layer was cured, and then another 100 μm was tape cast and cured. The alumina green body was sintered, and Figs. 11(a) and (b) show the fracture surface of the two-layer alumina part. The interface of the layer is not visible as shown in Fig. 11(b).

(C) Silicon Nitride: Silicon nitride has a high refractive index, n = 2.1, which resulted in poor cure depths when dispersed in the aqueous UV-curable solution. At 0.10 solids loading in the solution with n = 1.382, the cure depth was only 21 μm, and the cure depth decreased to 10 μm at a 0.20 solids loading. Even though a fluid 0.50 volume fraction silicon nitride suspension was achievable, the system was not studied further because of the low cure depth behavior.

Table IV. Cure Depth for 0.50 Solids Loading Alumina Dispersed in Aqueous UV-Curable Solutions

Alumina	Ultraviolet-curable aqueous solution	Cure depth (μm)	
		1500 mJ/cm^2	5170 mJ/cm^2
AKP-50 (d = 0.46 μm)	Aqueous 1 (n = 1.382)	400 ± 25	
AKP-15 (d = 0.61 μm)	Aqueous 1 (n = 1.382)	300 ± 25	400 ± 30
Reynolds (d = 0.34 μm)	Aqueous 4 (n = 1.418)	450 ± 30	600 ± 30

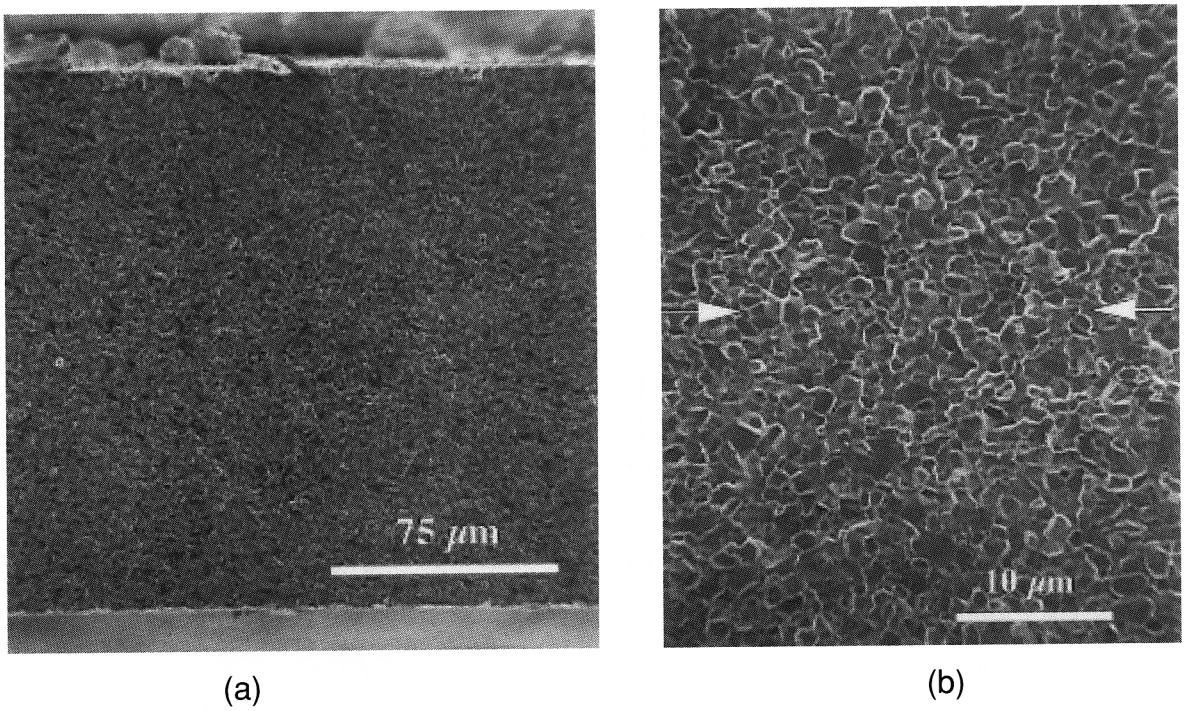

Fig. 11. (a) Low-magnification micrograph of fracture surface for sintered two-layer alumina part. (b) High-magnification micrograph showing the interface of the individual layers which cannot be resolved.

Figure 6 shows the cure depth versus inverse solids loading in the diacrylate, where $\Delta n^2 = 0.413$, a 11% decrease from the aqueous suspension. At 0.30 solids loading, the cure depth was 60 μm, an improvement over the aqueous suspension but well below the necessary 200 μm.

(3) SLA Silica Parts

For the fabrication of the first ceramic green body using stereolithography, 0.50 volume fraction silica was dispersed in the aqueous solution with $n = 1.418$ (see Fig. 7). Figure 12 shows the first silica box fabricated by stereolithography. This 136-layer box was built in about 4 h, where each layer was 150 μm thick. Because of time requirements, the box was started 0.635 cm (1/4 in.) from the bottom of the design; therefore, in the z-direction the box should be 1.905 cm (3/4 in.) tall. Note, the sides and the 45° angle were built accurately, where the x and y dimensions were 2.545 cm (1.002 in.) each. This represents an error of 50 μm, which can easily be compensated for during the laser scanning sequence.

Figure 13 shows a side view of the two silica boxes fabricated on the SLA-250. At the beginning of build, the layers curled because of polymerization shrinkage. This is most likely due to the laser draw style[27] where the polymerization shrinkage and curl behavior can be minimized by the choice of scanning sequence or space filling routine. The simple draw style chosen for the first attempt promoted curl in the beginning of the build which was evident until the 20th layer, after which the cured body was sufficiently rigid so the new polymerizing layer cannot cause further distortion. Subsequent research will determine the correct scanning sequence (SLA work performed over a 3 day period at 3D Systems in Valencia, CA).

The box tops are slightly rounded because the recoat blade was not used during the fabrication of the parts (modified resin vat for small suspension volume). After a layer was cured, the support platform was lowered into the fluid suspension, and the new layer flowed on top of the cured layer. Time was allowed for the suspension to equilibrate, creating a smooth layer ready

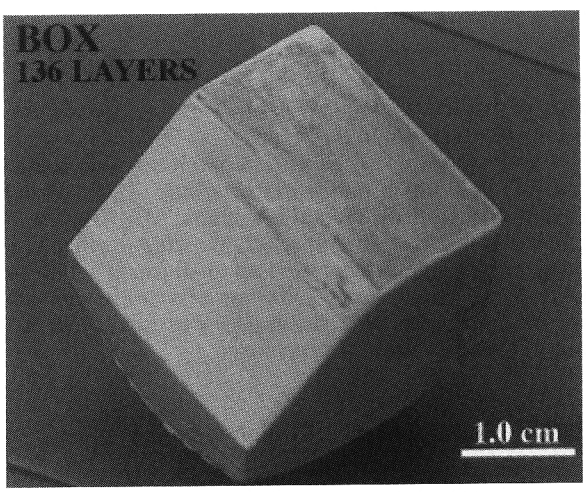

Fig. 12. First stereolithography part built using Michigan ceramic stereolithography suspension. Ceramic green body is 0.50 volume fraction silica cured in aqueous gel ($n = 1.418$). Box consists of 136 layers, each 150 μm thick.

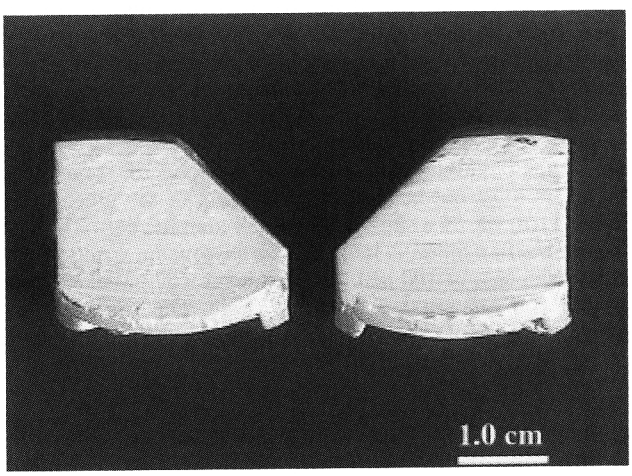

Fig. 13. Side view of two silica boxes built on SLA. Curl behavior is apparent at the beginning of build due to scanning style of the laser, whereas the slightly rounded tops are due to no recoat step during fabrication. The sides and 45° angles were accurately built.

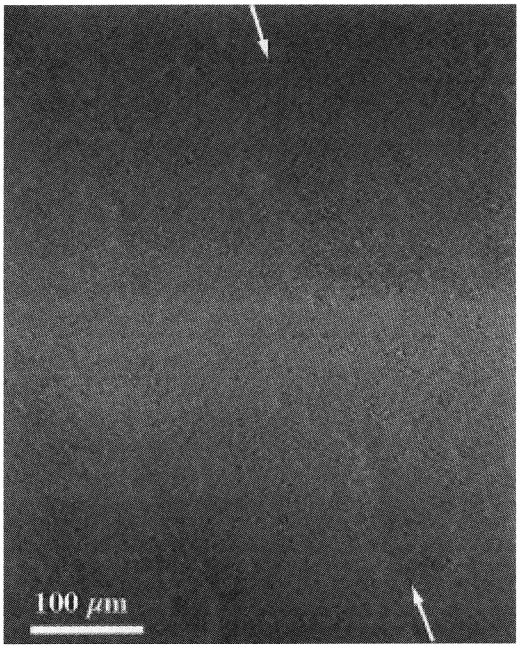

Fig. 14. Micrograph of silica box exterior, showing "knitting" of three layers. The arrows represent the interface of two layers, where the layers are not distinguishable.

for exposure. A time of 45 s was insufficient for the layers of the box top to equilize to a flat layer.

Figure 14 shows the adhesion between the individual layers for the silica box. Arrows point to a possible layer interface, but the interface is barely distinguishable. Note, in the picture there should be three layer interfaces which are not visible. Therefore, there is no problem with knitting the layers in the photopolymerization of a highly concentrated ceramic suspensions.

(4) Theory

The curing behavior of ceramic suspension can be modeled with Eqs. (1) and (2), which are derived and discussed in detail elsewhere.[9] Three linear relationships are expected for highly concentrated suspensions which scatter radiation. First, the cure depth should be linearly proportional to the logarithm of the exposure dose, and previous figures (Figs. 7 and 8) show this behavior. Note, for the SLA curves, only the large exposure dose regions are considered because this is the scattering limited region. Secondly, the cure depth should be inversely proportional to the volume fraction solid, $1/\phi$. Figure 6 shows C_d vs $1/\phi$ for a variety of ceramic suspensions, for silica and two alumina powders in the aqueous acrylamide solution, and silicon nitride in the diacrylate. All the data have a reasonably linear fit. Although we could not prepare a fluid 0.50 volume fraction silicon nitride suspension in the diacrylate, we can predict that the cure depth at this volume fraction should be $C_d = 40$ μm. Thirdly, cure depth should be inversely proportional to the square of the refractive index difference, Δn^2. Figure 15 shows the cure depth of 0.50 volume fraction silica in five aqueous solutions as a function of the inverse of the refractive index difference, $1/\Delta n^2$, demonstrating a good linear fit.

Particle size should play an important role, since it is well known that the particle size influences the scattering of the radiation.[28,29] The behavior of highly concentrated suspensions is not well understood. Figure 6 showed the cure depth increased for the smaller particle size alumina. We have not been able to reconcile this with simple scattering theories, such as Rayleigh-Gans or Mie theory, which relate the scattering to particle size for very dilute suspensions. For these highly concentrated suspensions, however, we find empirically that it is the ratio of the interparticle spacing (S) to the wavelength of the radiation (λ) that influences the cure depth, where $\beta = S/\lambda$. The scattering equation (Eq. (1)) using $Q = (S/\lambda)(\Delta n^2)$,

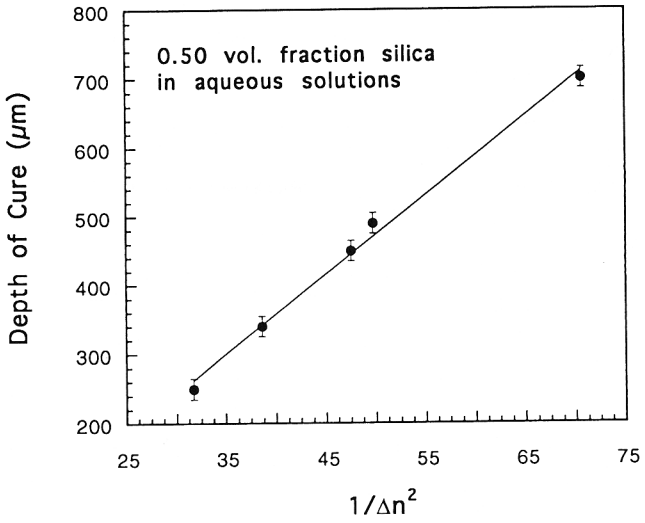

Fig. 15. Cure depth versus refractive index difference for 0.50 volume fraction silica dispersed in five aqueous UV-curable solutions.

accurately predicts the magnitude of the cure depth for these concentrated ceramic suspensions. Full details describing the theory and prediction of cure behavior for concentrated ceramic suspensions are described elsewhere.[9]

IV. Conclusions

Freeform fabrication of ceramics can be done with stereolithography using concentrated suspensions of powder in photopolymerizable media. Aqueous acrylamide-based suspensions have been demonstrated for alumina and for silica with viscosities below 500 mPa·s and cure depths above 300 μm at a dose of 1500 mJ/cm^2. These are adequate for useful fabrication by stereolithography. An acrylamide suspension of silicon nitride was fluid, but had insufficient depth of cure. Nonaqueous diacrylate-based suspensions have higher cure depths, but higher viscosities.

The first ceramic stereolithography part was built from a 0.50 volume fraction silica suspension in the aqueous acrylamide system using an SLA-250 with an Ar ion laser. This part was a box-shaped component with 136 layers, each 150 μm thick. Interlayer adhesion was adequate. Stereolithography test parts from alumina in the diacrylate system readily sintered to full density at 1550°C. Interlayer boundaries could not be distinguished in the sintered alumina.

Depth of cure can be modeled with a modified Beer–Lambert law, assuming scattering to be the primary mechanism. Cure depth is proportional to the logarithm of dose, inversely proportional to volume fraction ceramic, and inversely proportional to the square of the refractive index difference between the ceramic powder and the medium.

Acknowledgments: We wish to thank Dr. Paul Jacobs, Dr. Thomas Pang, and Kelly Kwo, at 3D Systems, for their time and use of their stereolithography apparatus.

References

[1]U. Lakshminarayan, S. Ogrydiziak, and H. L. Marcus, "Selective Laser Sintering of Ceramic Materials"; pp. 16–26 in Proceedings of the Solid Free Form Fabrication Symposium (Austin, TX, August 1990). Edited by H. L. Marcus *et al.* University of Texas, Austin, TX, 1990.

[2]M. J. Cima and E. M. Sachs, "Three Dimensional Printing: Form, Materials, and Performance"; pp. 187–94 in Proceedings of the Solid Free Form Fabrication Symposium (Austin, TX, August 1991). Edited by H. L. Marcus *et al.* University of Texas, Austin, TX, 1991.

[3]P. F. Jacobs, "Stereolithography 1993: Epoxy Resins, Improved Accuracy, and Investment Casting"; pp. 249–62 in Proceedings of the Fourth International Conference on Rapid Prototyping (Dayton, OH, June 1993). Edited by R. Chartoff *et al.* University of Dayton, Dayton, OH, 1993.

[4]M. Burns, *Automated Fabrication: Improving Productivity in Manufacturing*; pp. 40–43, 49–53. Prentice Hall, Englewood Cliffs, NJ, 1993.

[5]P. F. Jacobs, *Rapid Prototyping and Manufacturing: Fundamentals of Stereolithography*; pp. 1–23. Society of Manufacturing Engineers, Dearborn, MI, 1992.

[6]C. Hull, "Apparatus for Production of Three-Dimensional Objects by Stereolithography," U.S. Pat. No. 4 575 330, 1986.

[7]P. F. Jacobs, *Rapid Prototyping and Manufacturing: Fundamentals of Stereolithography*; pp. 11–18. Society of Manufacturing Engineers, Dearborn, MI, 1992.

[8]Dr. Paul Jacobs, Director of Research and Development, 3D Systems, Valencia, CA; private communication.

[9]M. Griffith; Ph.D. Thesis, Ch. 6. University of Michigan, Ann Arbor, MI, March 1995.

[10]S. P. Pappas, "Radiation Curing—A Personal Perspective"; pp. 1–20 in *Radiation Curing: Science and Technology.* Edited by S. P. Pappas. Plenum Publishing, New York, 1992.

[11]E. D. Pawlik, *Handbook of Optical Constants of Solids*; pp. 749–64, 771–74. Harcourt Brace Jovanovich, New York, 1985.

[12]C. L. Haertling, S. Yoshikawa, and R. R. Newnham, "Thick Film Patterned Ceramics Using UV-curable Pastes," *J. Am. Ceram. Soc.*, **73** [11] 3330–44 (1990).

[13]A. C. Young, O. O. Omatete, M. A. Janney, and P. A. Menchofer, "Gelcasting of Alumina," *J. Am. Ceram. Soc.*, **74** [13] 612–18 (1991).

[14]O. O. Omatete, M. A. Janney, and R. A. Strehlow, "Gelcasting—A New Ceramic Forming Process," *Am. Ceram. Soc. Bull.*, **70** [10] 1641–49 (1991).

[15]P. F. Jacobs, *Rapid Prototyping and Manufacturing: Fundamentals of Stereolithography*; pp. 27–281. Society of Manufacturing Engineers, Dearborn, MI, 1992.

[16]D. Meyers, "Colloids and Colloidal Stability"; p. 187–220 in *Surfaces, Interfaces, and Colloids.* VCH Publishing, New York, 1990.

[17]R. J. Hunter, *Foundations of Colloid Science*; pp. 329–447. Clarendon Press, Oxford, England, 1986.

[18]M. J. Crimp, R. E. Johnson, J. W. Halloran, and D. L. Feke, "Colloidal Behavior of SiC and Si_3N_4"; pp. 539–49 in *Science of Ceramic Chemical Processing*. Edited by L. L. Hench and D. R. Ulrich. Wiley, New York, 1986.

[19]S. G. Malghan, "Dispersion of Si_3N_4 Powders: Surface Chemical Interactions in Aqueous Media," *J. Colloid Surf.*, **62**, 87–99 (1992).

[20]F. H. Baader, T. J. Graule, and L. J. Gaukler, "Rheology of Concentrated Aqueous Alumina Suspensions"; to be published in the Proceedings of the 8th CIMTECH–World Ceramic Congress and Forum on New Materials (Florence, Italy, June 1994).

[21]Th. Tadros, "Rheology of Highly Concentrated Suspensions"; pp. 71–87 in *Advances in Fine Particle Processing*. Edited by J. Hanna and Y. A. Attia. Elsevier Science Publishers, New York, 1990.

[22]F. M. Fowkes, "Dispersions of Ceramic Powders in Organic Media"; pp. 411–21 in Advances in Ceramics, Vol. 21, *Ceramic Powder Science*. Edited by G. L. Messing, K. S. Mazdiyasni, J. W. McCauley, and R. A. Haber. American Ceramic Society, Westerville, OH, 1987.

[23]J. P. Foussier, "An Introduction to the Basic Principles in UV Curing"; pp. 49–117 in *Radiation Curing in Polymer Science and Technology*, Vol. I. Edited by J. P. Foussier and J. F. Rabek. Elsevier Applied Science, London, England, 1993.

[24]Dr. Douglas Neckers, Bowling Green State University, Photochemistry Department; private communication.

[25]J. P. Foussier, "Excited-State Reactivity in Radiacal Polymerisation Photoinitiators"; pp. 1–61 in *Radiation Curing in Polymer Science and Technology.* Vol. II. Edited by J. P. Foussier and J. F. Rabek. Elsevier Applied Science, London, England, 1993.

[26]C. Decker and K. Moussa, "UV-Radiation and Laser-Induced Polymerization of Acrylic Monomers"; pp. 439–56 in ACS Symposium Series, No. 417, *Radiation Curing of Polymeric Materials*, Proceedings of the American Chemical Society. American Chemical Society, Washington, DC, 1990.

[27]S. Ulett, R. P. Chartoff, A. J. Lightman, J. P. Murphy, and J. Li, "Reducing Warpage in Stereolithography through Novel Draw Styles"; pp. 242–89 in Proceedings of the Solid Free Form Fabrication Symposium (Austin, TX, August 1994). Edited by H. L. Marcus *et al.* University of Texas, Austin, TX, 1994.

[28]H. C. van de Hulst, *Light Scattering by Small Particles*. Wiley, New York, 1957.

[29]P. W. Barber and S. C. Hill, *Light Scattering by Particles: Computational Methods*. World Scientific Publishing, Teaneck, NJ, 1990. □